

This is the **accepted version** of the article:

Vila, Bernat; Sellés, Albert G; Moreno Azanza, Miguel; [et al.]. «A titanosaurian sauropod with Gondwanan affinities in the latest Cretaceous of Europe». *Nature Ecology & Evolution*, (February 2022). DOI 10.1038/s41559-021-01651-5

This version is available at <https://ddd.uab.cat/record/254843>

under the terms of the  **CC BY** COPYRIGHT license

A titanosaurian sauropod with Gondwanan affinities in the latest Cretaceous of Europe

Bernat Vila*^{1,2}, Albert Sellés^{1,2}, Miguel Moreno-Azanza^{3,4,5}, Novella L. Razzolini^{1,2},
Alejandro Gil-Delgado^{2,6}, José Ignacio Canudo⁵, Àngel Galobart^{1,2}

1. Institut Català de Paleontologia Miquel Crusafont, Universitat Autònoma de Barcelona, Carrer Escola Industrial 23, 08201 Sabadell (Barcelona), Catalonia, Spain.

2. Museu de la Conca Dellà, Carrer del Museu, 4, Isona (Lleida), Catalonia, Spain.

3. GEOBIOTEC, Department of Earth Sciences, NOVA School of Science and Technology, Universidade Nova de Lisboa, 2829-516, Caparica, Portugal.

4. Espaço NovaPaleo, Museu de Lourinhã, Rua João Luís de Moura 95, 2530-158, Lourinhã, Portugal.

5. Grupo Aragosaurus-IUCA, Paleontología, Facultad de Ciencias, Universidad de Zaragoza, Calle Pedro Cerbuna, 12, 50009 Zaragoza, Spain.

6. Departament de Geologia, Facultat de Ciències, Universitat Autònoma de Barcelona, 08193 Cerdanyola del Vallès (Barcelona), Spain.

Corresponding author: bernat.vila@icp.cat

ORCID IDs: BV, [0000-0002-5935-1732](https://orcid.org/0000-0002-5935-1732); AGS, [0000-0002-4637-6084](https://orcid.org/0000-0002-4637-6084); MMA, [0000-0002-7210-1033](https://orcid.org/0000-0002-7210-1033); NR, [0000-0002-2234-8935](https://orcid.org/0000-0002-2234-8935); AG-D, 0000-0001-5147-5426; JIC, [0000-0003-1732-9155](https://orcid.org/0000-0003-1732-9155); AG, [0000-0003-1508-4561](https://orcid.org/0000-0003-1508-4561).

1 **ABSTRACT**

2 The origin of the last sauropod dinosaur communities in Europe and their evolution
3 during the final 15 million years of the Cretaceous has become a complex
4 phylogenetic and palaeobiogeographic puzzle characterized by the controversy on
5 the alleged coexistence of immigrant, Gondwana-related taxa alongside relictual and
6 insular clades. In this context, we describe a new titanosaurian sauropod dinosaur,
7 *Abditosaurus kuehnei* gen. et sp. nov., from the Upper Cretaceous (Maastrichtian)
8 Tremp Group of Catalonia (Spain). Phylogenetic analyses recover *Abditosaurus*
9 separately from other European titanosaurs, within a clade of otherwise South
10 American and African saltosaurines. The affinity of the new taxon with southern
11 landmasses is reinforced by spatiotemporal co-occurrence with Gondwanan
12 titanosaurian oospecies in southern Europe. The large size and the lack of
13 osteohistological features potentially related to insular dwarfism or size reduction
14 support the idea that *Abditosaurus* belongs to an immigrant lineage, unequivocally
15 distinct from some of the the island dwarfs of the European archipelago. The arrival
16 of the *Abditosaurus* lineage to the Ibero-Armorican island is hypothesized to have
17 occurred during the earliest Maastrichtian (70.6 Ma), probably as a result of a global
18 and regional sea-level drop that reactivated ancient dispersal routes between Africa
19 and Europe. The arrival of large-bodied titanosaurs to the European archipelago
20 produced dramatic changes in its insular ecosystems and important evolutionary
21 changes in its dinosaur faunas, especially with respect to the 'island rule' effect.

22

23 INTRODUCTION

24 At the very end of the Cretaceous, Europe was an extensive island archipelago in
25 which titanosaurian sauropods were integral components of terrestrial ecosystems.
26 In the large Ibero-Armorican Island (which included the current areas of south-
27 western France, Spain, and Portugal), the evolution of sauropod communities was
28 shaped by the “Maastrichtian Dinosaur Turnover”, a major faunal change in which
29 the late Campanian–early Maastrichtian (LC–EM) pre-turnover dinosaur
30 communities were replaced by early–late Maastrichtian post-turnover assemblages^{1–}
31 ³. The pre-turnover titanosaur assemblage included small-sized species such as
32 *Lirainosaurus astibiae*, *Atsinganosaurus velauciensis*, and *Garrigatitan meridionalis*^{4–}
33 ⁶, and moderate-sized species such as *Ampelosaurus atacis* and *Lohuecotitan*
34 *pandafilandi*^{7,8}, some of which have been interpreted to have lowered metabolic
35 rates^{6,9–11}. Reduction of body size and shifts in growth rate relative to their
36 contemporaneous sister taxa from continental landmasses may have resulted from
37 selective pressures under insular, limited-resource environments – an evolutionary
38 process known as insular dwarfism^{12,13}. In contrast, the post-turnover forms are
39 apparently larger in size but still taxonomically undescribed^{14,15}, and their first
40 appearance on the island co-occurs with a specific group of oospecies of
41 Gondwanan affinity. Recent phylogenetic analyses distinguish two distinct clades: a
42 relictual core of endemic titanosaurs, and a clade of immigrants with African
43 affinities¹¹. This partially supports a previously-postulated biotic interchange,
44 including sauropod faunas, between the archipelago – mostly and particularly with
45 the Ibero-Armorican Island¹⁶ – and the neighbouring landmasses during the latest
46 Cretaceous^{17–21}.

47 Here we present a new titanosaurian sauropod dinosaur from the Late Cretaceous
48 (Maastrichtian) of Catalonia that represents the most complete, semi-articulated
49 titanosaur skeleton thus far discovered in Europe. Phylogenetic analyses of this
50 informative taxon provide an opportunity to test hypotheses of phylogenetic
51 relationships among European titanosaurs and shed light on palaeobiogeographic
52 events between the southern islands of the European archipelago and the northern
53 regions of the African landmass. Further, the new taxon is substantially larger-bodied
54 than any species within the late Campanian–early Maastrichtian titanosaur
55 assemblage, probably indicating an eventual decrease of the alleged insular
56 dwarfism or the so-called ‘island rule’ effect in Ibero-Armorican sauropod faunas.

57

58 **RESULTS**

59 **Nomenclatural acts**

60

61 **Systematic palaeontology**

62 DINOSAURIA Owen, 1842

63 SAURISCHIA Seeley, 1887

64 SAUROPODA Marsh, 1878

65 TITANOSAURIA Bonaparte and Coria, 1993

66 SALTASAURIDAE Bonaparte and Powell, 1980

67 SALTASAURINAE Bonaparte and Powell, 1980

68 ***Abditosaurus kuehnei***, gen. et sp. nov.

69

70 The Life Science Identifiers (LSIDs) for this publication are:

71 [urn:lsid:zoobank.org:act:C9CDB600-42D3-4448-910F-5630DEA64A90](https://zoobank.org/urn:lsid:zoobank.org:act:C9CDB600-42D3-4448-910F-5630DEA64A90);

72 [urn:lsid:zoobank.org:act:D9EFD886-7FE2-440C-AAC2-C8C88DF035A3](https://zoobank.org/urn:lsid:zoobank.org:act:D9EFD886-7FE2-440C-AAC2-C8C88DF035A3)

73

74 **Etymology** – ‘*Abditus*’, Latin, concealed, because the skeleton was concealed from

75 science for 60 years; ‘*sauros*’, Greek, lizard. ‘*kuehnei*’ honours Professor Walter

76 Georg Kühne (1911–1991), the discoverer of the specimen.

77 **Holotype** – An associated, semi-articulated, partial skeleton consisting of isolated

78 teeth, 12 articulated and partial cervical vertebrae, cervical ribs, seven nearly

79 complete or fragmentary anterior and middle dorsal vertebrae, six complete or

80 almost complete dorsal ribs and fragments of others, three chevrons, the right

81 scapula, posterior end of the left scapular blade, right coracoid, left sternal plate, a

82 sternal rib, proximal half of the left humerus, distal half of the right humerus, partial

83 right radius, fragment of the left ilium, part of the proximal half of the right femur, right

84 tibia, right fibula, and distal half of the left fibula with the adhered calcaneum (see

85 Supplementary Section 2.1 for a list of materials with repository numbers). We

86 consider these elements to represent a single titanosaurian individual because they

87 formed a partially articulated skeleton within an accumulation area of 6 m by 4 m at

88 the same stratigraphic level. No duplicated elements were found (Fig. 1).

89 **Type locality** – Orcau-1, approximately 6 km east of Tremp, Pallars Jussà county,

90 Catalonia, Spain (Fig. 1; coordinates: 42° 9' 34.1424" N, 0° 58' 22.631" E). The

91 locality (formerly known as “Barranco de Orcau” or “Orcau”) was discovered in 1954

92 by Walter Georg Kühne during fieldwork in the Suterranya-Orcau area (see

93 Supplementary Section 2.1).

94 **Horizon** – Lower portion of the Tremp Group, basalmost strata of the Conques
95 Formation³. Other fossils identified at the Orcau-1 locality include shed
96 crocodylomorph teeth (MCD-6752), plant remains, and *Lychnus* gastropod casts.
97 Two isolated, shed dromaeosaurid teeth (MCD-6994, MCD-6740) and scattered
98 eggshells (*Fusiolithus baghensis*; IPS59133²²) were found in a stratigraphic level
99 immediately above the sauropod skeleton.

100 **Age and distribution** – ca. 70.5 Ma, early Maastrichtian (C31r), Late Cretaceous³.

101 **Diagnosis** – *Abditosaurus kuehnei* is diagnosed by a unique combination of
102 characters not seen in other titanosaurs as well as 14 autapomorphies (marked with
103 an asterisk): anterior dorsal vertebrae with anterior centrodiapophyseal lamina (acdl)
104 not reaching centrum but intersecting centroprezygapophyseal lamina (cpri)*;
105 anterior and first middle dorsal vertebrae with diapophyses ventral to
106 postzygapophyses*, absence of centroprezygapophyseal lamina (cpri)*, and long
107 axes of zygapophyses at low angle relative to horizontal plane (the latter character
108 shared with *Argentinosaurus*²³); middle dorsal vertebrae with oblique,
109 posterodorsally oriented accessory lamina dividing parapophyseal
110 centrodiapophyseal fossa (pacdf)*, secondary prezygodiapophyseal lamina (prdl)
111 dividing prezygapophyseal paradiapophyseal fossa (prpadf)*, posterior
112 centrodiapophyseal lamina (pcdl) dorsally penetrated by large pneumatic foramen
113 (shared with *Rapetosaurus*²⁴, *Lohuecotitan*⁸, and *Saltasaurus*²⁵), abundant
114 pneumatic foramina in spinopostzygapophyseal (spof)*, centropostzygapophyseal
115 (cpof)*, and postzygapophyseal centrodiapophyseal (pocdf)* fossae, pneumatized
116 centropostzygapophyseal lamina (cpol) (shared with *Rapetosaurus*²⁴), and absence
117 of postspinal laminae (posl) (shared with *Overosaurus*²⁶, *Muyelensaurus*²⁷, and
118 *Isisaurus*²⁸); anterior dorsal ribs without pneumatic foramina on anterolateral and

119 posteromedial surfaces*; second dorsal ribs with anteroposterior thickening or bulge
120 on posterior margin of distal end*; scapula with co-occurrence of posteroventral
121 process or tubercle on medial margin of acromial plate, subtle process on
122 anteroventral corner, and very prominent bulge on dorsomedial margin of blade, and
123 two oval lateral fossae on posterior end of blade*; coracoid with elliptical foramen
124 that twists its orientation from lateral through to medial surface*; sternal plate without
125 anteroventral ridge on ventral surface (shared with *Mnyamawamtuka*²⁹); presence of
126 sternal ribs; humerus with a medially projected deltopectoral crest (shared with
127 *Gondwanatitan*³⁰, *Nullotitan*³¹, and *Jainosaurus*³²) and articular surface of radial
128 condyle facing anterodistally (shared with *Saltasaurus*³³ and *Paralititan*³⁴); radius
129 with oblique ridge on posterodistal surface*; tibia with anteriorly projected cnemial
130 crest (shared with *Gondwanatitan*³⁰) and small prominent bulge at posterior margin
131 of proximal end (shared with *Neuquensaurus*³⁵); fibula with distal end beveled
132 posteriorly 20° with respect to long axis of shaft*; presence of ossified calcaneum
133 (shared with *Neuquensaurus*³⁶ and presumably with *Elaltitan*³⁷).

134

135 **Osteological description and comparisons** – The **cervical** vertebrae (Fig. 2a)
136 have opisthocoelous, internally pneumatized centra with ventral surfaces lacking a
137 ventral keel or ventrolateral ridges, thus differing from all or some of the cervical
138 centra of most titanosaurs such as *Lohuecotitan*⁸, *Rapetosaurus*²⁴, *Saltasaurus*²⁵,
139 and *Overosaurus*²⁶, which bear some of these structures. Unlike most titanosaurs,
140 the posterior cervical centra bear large, oval, and deep pleurocoels. The
141 parapophyses extend half the anteroposterior length of the centrum, project laterally,
142 and are located on the anterior margin of the centrum, as in most titanosaurs. The
143 neural spine is estimated to be short. **Cervical ribs** are fused in nine of the 12

144 cervical vertebrae and project far laterally from the centrum (Fig. 2a). The anterior
145 process has a projection that curves medially, resembling a characteristic 'batwing'
146 shape, and extends to the level of the anterior margin of the condyle. The posterior
147 process is elongate and thins distally, overlapping 2.5 more posterior centra. The
148 **dorsal vertebrae** are described with the neural canal oriented horizontally. They are
149 strongly opisthocoelous, have camellate internal tissue, and become shorter from the
150 anterior to the middle vertebrae (Fig. 2b and c). All centra lack a ventral keel, and the
151 lateral pleurocoels are oval and undivided. In the anterior and first middle dorsal
152 vertebrae, the transverse processes are low (with the ventral edge approximately
153 level with the dorsal edge of the posterior cotyle) and laterally directed, as in
154 *Lohuecotitan*⁸ and other titanosaurs^{23,24,28}. In the anterior dorsal vertebrae, the
155 anterior centrodiapophyseal lamina does not reach the centrum because it intersects
156 the centroprezygapophyseal lamina. The neural spine is large and triangular,
157 moderately tall, and angled posterodorsally (Fig. 2b), like those of the middle dorsal
158 vertebrae of most European titanosaurs and others. The surfaces of the
159 spinopostzygapophyseal, centropostzygapophyseal, and postzygapophyseal
160 centrodiapophyseal fossae are autapomorphically pneumatized by scattered
161 foramina. The intrapostzygapophyseal and postspinal laminae are absent, as in
162 *Overosaurus*²⁶. The long axes of the zygapophyses are at a low angle relative to the
163 horizontal plane, as in *Argentinosaurus*²³, and the diapophyses are laterally directed
164 and located at level with the prezygapophyses. *Abditosaurus* is unique in having the
165 diapophyses ventral to the postzygapophyses in the anterior and first middle dorsal
166 vertebrae (first, second, and third dorsals) (Fig. 2b). A secondary
167 prezygodiapophyseal lamina in the first middle dorsal and a parapophyseal
168 centrodiapophyseal fossae internally divided by an oblique, posterodorsally-oriented

169 accessory lamina in the middle dorsals are two autapomorphies of *Abditosaurus*.
170 Unlike in other Ibero-Armorican species and many other titanosaurs, the
171 centroprezygapophyseal lamina is absent. The posterior centrodiapophyseal lamina
172 bears a dorsal and elliptical pneumatic foramen (Fig. 2b,c), a character shared with
173 *Lohuecotitan*⁸, *Rapetosaurus*²⁴, and *Saltasaurus*²⁵. The capitulum and tuberculum of
174 the **dorsal ribs** (Fig. 2d) are oriented at a right angle and united by a thin
175 capitulotubercular web that shows camellate texture. The web lacks pneumatic
176 foramina, unlike most titanosauriforms³⁸, a feature that we regard as a local
177 autapomorphy of *Abditosaurus*. The rib head bears a proximodistally elongate and
178 narrow ridge (outstandingly pronounced in the third rib) that extends distally from the
179 tuberculum onto the rib shaft. The rib shaft has a plank-like, asymmetric, D-shaped
180 cross-section. The second through fourth ribs show a distal spoon-like expansion. In
181 the third dorsal rib, this expansion produces a distal peduncle where the rib
182 articulates with the sternal plates. Autapomorphically, the posterior surface of the
183 distal end of the second ribs bears a striated anteroposterior thickening or bulge.
184 Caudal **chevrons** (Fig. 2e) are dorsally open and ‘Y-shaped’ with rounded to oval
185 articular facets. The middle chevron has two dorsal articular subfacets, but unlike
186 *Lohuecotitan*⁸ they lack a distinct groove between them.
187 The **scapula** is described with the scapular blade oriented horizontally. The acromion
188 and acromial ridge are oriented perpendicular to the long axis of the blade and dorsally
189 expanded to twice the dorsoventral breadth of the posterior end (Fig. 2f). The scapular
190 blade has a nearly ‘D’-shaped cross section at its anterior end and lacks a ventral
191 ridge on the medial surface, unlike *Atsinganosaurus*¹¹, *Lirainosaurus*³⁹,
192 *Ampelosaurus*⁴⁰, *Mansourasaurus*¹⁶, and *Opisthocoelicaudia*⁴¹. Posteriorly, the
193 posterodorsal expansion is more pronounced than the posteroventral expansion, as

194 in several titanosaurs but differing from *Lirainosaurus*³⁹ and *Ampelosaurus*⁴⁰, among
195 others. The posterior end of the scapular blade bears two autapomorphic lateral
196 fossae or depressions. The co-occurrence of a posteroventral process on the medial
197 margin of the acromial plate, a subtle process on the anteroventral corner, and a very
198 prominent bulge on the dorsomedial margin of the scapular blade is unique to
199 *Abditosaurus*. The scapula contributes more to the glenoid than does the coracoid,
200 differing from *Lirainosaurus* (coracoid contributes more than scapula³⁹) and
201 *Opisthocoelicaudia* (scapula and coracoid contributes subequally⁴¹), but similar to
202 *Mansourasaurus*¹⁶. The **coracoid** is described with the glenoid surface oriented
203 posteroventrally (Fig. 2g). It is longer than tall and has a quadrangular outline, a
204 character shared with several titanosaurs, and as in many of these sauropods it lacks
205 a ridge originating near the midpoint of the anterodorsal border of the lateral surface.
206 The coracoid foramen is far from the scapular articulation, as in several titanosaurs,
207 but differing from *Atsinganosaurus*¹¹, *Lirainosaurus*³⁹, *Ampelosaurus*⁴⁰, and some
208 other derived titanosaurs^{16,24,42}. The foramen is elliptical and autapomorphically twists
209 its orientation from the lateral through to the medial surface. In articulation with the
210 scapula, the dorsal margin of the coracoid is situated below the level of that of the
211 scapular acromial plate. The **sternal plate** (Fig. 2h) is semilunar, with a strongly
212 concave lateral surface, as in other titanosaurs^{43,44}. Unlike most titanosaurs⁶,
213 however, it lacks an anteroventral ridge on the ventral surface (as in
214 *Mnyamawamtuka*²⁹). The ratio of the length of the sternal plate to that of the humerus
215 is 0.68 in *Abditosaurus*, which falls very close to the value seen in saltasaurids
216 (>0.7)⁴⁴. The **sternal rib** (Fig. 2i) is elongate and rod-like and challenges the
217 assumption that the loss of ossified sternal ribs might be a synapomorphy of
218 Titanosauriformes⁴⁵. The presence of this element in *Abditosaurus* is considered a

219 local autapomorphy within the clade. The ossification of at least one sternal rib in the
220 new form might be related to the very advanced ontogenetic age of the holotypic
221 individual.

222 The **humerus** (Fig. 2j and k) is robust and remarkably different from the more gracile
223 humeri of Ibero-Armorican and many other titanosaurs. The mediolateral
224 development of the proximal end is similar to those described in *Saltasaurus*³³,
225 *Neuquensaurus australis*³⁵, and *Opisthocoelicaudia*⁴¹. The deltopectoral crest is
226 robust and strongly expanded mediolaterally to reach the central axis of the shaft, as
227 in several titanosaurs, but differs from the unexpanded or moderately expanded
228 crests of all other Ibero-Armorican taxa and many other titanosaurs. It projects
229 unambiguously medially, similar to *Gondwanatitan*³⁰, *Nullotitan*³¹, and *Jainosaurus*³².
230 Unlike other Ibero-Armorican titanosaurs, the *Abditosaurus* humerus exhibits a
231 distally expanded deltopectoral crest, a synapomorphy of Saltosauridae^{44,46} shared
232 with *Opisthocoelicaudia*⁴¹, *Saltasaurus*⁴⁷, *N. australis*⁴⁸, and *Alamosaurus*⁴⁹. The
233 distal condyles are clearly divided as in saltosaurids^{44,46}, and the articular surface of
234 the radial condyle faces anterodistally, as in *Paralititan*³⁴ and *Saltasaurus*⁴⁷. The
235 **radius** (Fig. 2l) has a mediolaterally expanded distal end that is beveled
236 posterolaterally more than 20° relative to the long axis of the shaft and a well-defined
237 interosseus ridge, as in other lithostrotian titanosaurs⁴⁴. The interosseous ridge
238 extends proximodistally and is laterally emarginated, as in *Opisthocoelicaudia*⁴¹.
239 Unlike the rounded shape of *Rapetosaurus*²⁴ or *Dreadnoughtus*⁵⁰, the distal surface
240 is elliptical and anteroposteriorly asymmetrical, as in *N. australis*⁴⁸.
241 Autapomorphically, *Abditosaurus* presents a small, oblique ridge on the posterodistal
242 surface of the radius.

243 The **ilium** has a preacetabular process that projects anterolaterally, as in
244 *Garrigatitan*⁶ and *Lohuecotitan*⁸ but differing from *Lirainosaurus*³⁹. Internally, it is
245 pneumatized, as in most Ibero-Armorican titanosaurs^{6,8,11,39}, *Alamosaurus*⁵¹,
246 *Saltasaurus*, and *Neuquensaurus*⁵², among others. The **femur** exhibits a prominent,
247 proximally located, lateral bulge as well as a posterior accessory ridge. The
248 eccentricity index of the shaft is >185%, as in most titanosaurs⁵³. The **tibia** (Fig. 2m)
249 is gracile, and its proximal end is less mediolaterally compressed than in
250 *Atsinganosaurus*¹¹ and *Lirainosaurus*³⁹, but also contrasting with the rounded shape
251 of *Lohuecotitan*⁸ and *Ampelosaurus*⁴⁰. A small but prominent bulge at the posterior
252 margin of the proximal end is also observed in *Neuquensaurus*³⁵, and the cnemial
253 crest projects anteriorly, as in *Gondwanatitan*³⁰. The distal end is longer
254 mediolaterally than anteroposteriorly, as typical for titanosaurs^{43,54}. The anteromedial
255 ridge is more pronounced than in *Lirainosaurus*³⁹, *Atsinganosaurus*¹¹, and
256 *Lohuecotitan*⁸. The sigmoid shape of the **fibula** (Fig. 2n) is a character shared with
257 most Campanian–Maastrichtian titanosaurs, and the presence of a prominent lateral
258 trochanter is a synapomorphy of Saltosaurinae⁴⁸. The fibula of *Abditosaurus* is
259 unique in having its distal end beveled posteriorly 20° with respect to the long axis.
260 The distal articular surface is triangular, as in *Rapetosaurus*²⁴, *Lirainosaurus*³⁹,
261 *Alamosaurus*⁵⁵, and *Laplatasaurus*⁵⁶. The **calcaneum** (Fig. 2o) is a small, convex,
262 and oval element, as in *Euhelopus*⁵⁷ and the purported calcaneum reported in
263 *Elaltitan*³⁷. The ossification of the calcaneum (and a sternal rib) in the *Abditosaurus*
264 holotype is exceedingly rare in Titanosauria, and therefore their presence in this
265 senescent individual might indicate that the preservation of these elements is related
266 to its advanced ontogenetic stage.

267

268 **DISCUSSION**

269 **Phylogenetic and palaeobiogeographic analyses**

270 We assessed the phylogenetic affinities of *Abditosaurus kuehnei* using both
271 parsimony and Bayesian methods with the dataset of Gorscak and O'Connor²⁹ (see
272 Methods and Supplementary Section 1.6). In both analyses, *Abditosaurus kuehnei* is
273 recovered as a saltosaurid lithostrotian titanosaur on the basis of the following
274 synapomorphies: coracoid with rectangular anteroventral margin; humerus with
275 strong posterolateral bulge around level of deltopectoral crest apex; humeral
276 deltopectoral crest expanded distally; humeral distal condyles divided; and radius
277 with distal end beveled ca. 20° proximolaterally relative to shaft⁴³. More specifically,
278 *Abditosaurus* is positioned within a clade of Late Cretaceous saltosaurines from
279 South America and Africa (Fig. 3). Within this otherwise South American–African
280 clade, *Abditosaurus* and *Paralititan* are sister taxa, and the *Abditosaurus* +
281 *Paralititan* clade is the sister taxon of *Maxakalisaurus*. The (*Abditosaurus* +
282 *Paralititan*) + *Maxakalisaurus* clade is the sister taxon of the South American
283 saltosaurins (*Saltasaurus* + *Neuquensaurus*). The South American–African clade as
284 a whole (that is, [*Paralititan* + *Abditosaurus*] + *Maxakalisaurus* and *Saltasaurus* +
285 *Neuquensaurus*) is supported by two synapomorphies (anterior and middle caudal
286 centra wider than tall; divided humeral distal condyles) and is sister to
287 Opisthocoelicaudiinae⁵⁹, a Pan-American, African, and Eurasian clade that
288 comprises most of the rest of the Ibero-Armorican taxa as well as the North
289 American *Alamosaurus*, the South American *Dreadnoughtus*, and the Asian
290 *Opisthocoelicaudia*, among others.

291 The phylogenetic and palaeobiogeographic analyses (Fig. 3) indicate that
292 *Abditosaurus* is a derived member of a distinct immigrant clade of otherwise South

293 American and African saltosaurine titanosaurs that reached Europe via a dispersal
294 event from Africa during the post-Cenomanian, very probably during the early
295 Maastrichtian. Further, the direct association of the *Abditosaurus* skeleton with
296 *Fusioolithus baghensis*, an oospecies with in-ovo titanosaur embryos⁶⁰ and an
297 otherwise Gondwanan (South America, India, Africa) distribution (see
298 Supplementary Section 2.4), reinforces the southern origin of the clade. The
299 dispersal event from Africa is hypothesized to have occurred during the KMa2
300 regressive event (70.6 Ma, early Maastrichtian), a eustatic event⁶¹ that affected the
301 central Tethyan margin and northern Africa. With the subaerial exposure of various
302 carbonate platforms, the Europe–Africa connection was reestablished, and Early
303 Cretaceous migratory routes⁶²⁻⁶⁴ were probably reactivated, facilitating the dispersal
304 of titanosaurian taxa (Fig. 4; Supplementary Section 2.6).

305

306 **Implications for titanosaur evolution in the European archipelago**

307 *Abditosaurus* was a large titanosaur by Ibero-Armorican standards, representing a
308 very mature, senescent, individual estimated to be 17.5 m in length with a body
309 mass of 14,053 kg (see Supplementary Table 1). Overall, it was substantially larger
310 than any titanosaur species described from the region, being more than 70% larger
311 than the largest known adult *Atsinganosaurus* and *Garrigatitan*, more than twice the
312 size of the largest individuals attributed to *Lirainosaurus* or *Lohuecotitan*, and 20%
313 larger than the largest individual attributed to *Ampelosaurus* (Supplementary Table
314 1). The anatomical and osteohistological characters of the senescent *Abditosaurus*
315 do not indicate a reduction in growth rate nor a reduction in body size (see
316 Supplementary Section 2.3), two common traits found in *Lirainosaurus*⁹,
317 *Ampelosaurus*¹⁰, *Atsinganosaurus*¹¹, and *Magyarosaurus*⁶⁶. Indeed, the

318 *Abditosaurus* appendicular bones lack modified laminar bone, a bone tissue
319 potentially related to a reduction in metabolic rate and body size¹⁰ and interpreted as
320 evidence for possible insular dwarfism in sauropods^{9-11,20}. Therefore, there is no
321 evidence for metabolic adaptations to insular settings in *Abditosaurus*, as are
322 present in other European titanosaurs^{13,66}. Our results suggest that *Abditosaurus*
323 must be regarded as a member of a distinct immigrant clade of large titanosaurs that
324 reached Ibero–Armorica during the early Maastrichtian, and as a representative of
325 the post-turnover titanosaurian fauna of this island.

326 The scenario during the middle of the early Maastrichtian (lower part of C31r) of
327 large-bodied, post-turnover titanosaurs in the Ibero-Armorican island replacing small
328 late Campanian–early Maastrichtian forms might be mirrored in other islands of the
329 European archipelago, such as in the eastern Hațeg Island (in modern-day
330 Romania), where large taxa seem to appear later than dwarfed forms (e.g.,
331 *Magyarosaurus*⁶⁷), probably also by the middle of the early Maastrichtian (lower part
332 of C31r⁶⁸). Accordingly, these new titanosaur faunas are expected to be associated
333 with fusioolithid oospecies in post-early Maastrichtian deposits. Hence, this proposed
334 titanosaurian faunal replacement might represent the decrease of the ‘island rule’
335 effect on sauropod communities throughout Europe.

336

337 **METHODS**

338 **Osteohistological analyses** - Histological samples were taken from the humerus,
339 femur, and tibia, prepared as thin sections, and studied using a petrographic
340 microscope. **Body mass and length estimates** - We compiled a dataset of limb
341 bone measurements for the Ibero-Armorican titanosaur species (Supplementary
342 Table 1) for use in body mass (BM) and body length (BL) estimations with the

343 formulas of Campione and Evans⁶⁹ based on femoral and humeral circumferences,
344 which were estimated following the allometric equation of González Riga et al.⁷⁰
345 when necessary, and Seebacher⁷¹. **Photogrammetric models** – 3-D models of
346 fossil specimens were produced following photogrammetric protocols⁷²⁻⁷⁴ and using
347 Agisoft Photoscan Pro (v. 1.2.4, www.agisoft.com), to perform scaling and alignment.
348 **Phylogenetic and palaeobiogeographic analyses** – We performed maximum
349 parsimony and Bayesian analyses. Maximum parsimony analyses used the dataset
350 of Gorscak and O'Connor²⁹, which included the original 55 taxa plus *Abditosaurus*
351 scored for 272 independent characters that were treated as unordered in all the
352 analyses. Both equal weights and extended implied weighting analyses with different
353 concavity constants were explored. The Bayesian dataset²⁹, which also included the
354 original 55 taxa plus *Abditosaurus*, was coded for a total of 272 variable characters
355 plus 260 autapomorphic, invariable characters. A non-clock analysis was carried out
356 using MrBayes 3.2.6⁷⁵, running in the CIPRES Science Gateway, using a model of
357 variable rates of character state change, sampled from a lognormal-distribution,
358 setting an exponential hyperprior of 1.0 for the rate of variation among characters.
359 Four independent runs of the Markov chain Monte Carlo (MCMC) ran for 10 million
360 generations with one hot and three cold chains. The chains sampled tree-space
361 every 1,000 generations and the first 25% of the posterior distribution was discarded
362 to eliminate the initial climbing phase. Convergence of independent runs was
363 assessed in Tracer 1.7 using effective sample size (ESS) for each parameter greater
364 than 200. We also performed a tip-dating Bayesian phylogenetic analysis to estimate
365 divergence dates and branch lengths based on the additional data in the form of
366 stratigraphic information. The assumed tree model for this set of analyses was the
367 birth-death-skyline-serial-sampling⁷⁶. A relaxed clock was assumed under a

368 lognormal distribution of sampled rates. Rates of character change were tested
369 under variable (with an assumed gamma-distribution) assumptions. Four
370 independent runs of the MCMC persisted for 50 million generations with sampling of
371 tree-space occurring every 1,000 generations and the first 25% of the sample was
372 discarded. Stratigraphic ranges of each taxon (see Supplementary Section 1.6 and
373 Table 2) were sampled under a uniform distribution to account for stratigraphic
374 uncertainty. Again, convergence of independent runs was assessed in Tracer 1.7
375 using effective sample size (ESS) for each parameter greater than 200. A
376 palaeobiogeographic analysis following the methodology of Sallam et al.¹⁶ was
377 conducted using the R script BioGeoBEARS⁷⁷ over the tip dating maximum clade
378 credibility tree. Three models (DEC, DIVALIKE, and BAYAREALIKE) and alternative
379 models with the additional + J parameter to facilitate long-distance dispersal events
380 alongside the assumptions of each model were evaluated. All figures were created
381 by the authors using Adobe Illustrator CC 2015 2.1.

382

383 **Data availability** –This published work and the nomenclatural acts it contains have
384 been registered in ZooBank, the proposed online registration system for the
385 International Code of Zoological Nomenclature (ICZN). The ZooBank LSIDs (Life
386 Science Identifiers) can be resolved and the associated information viewed through
387 any standard web browser by appending the LSID to the prefix “<http://zoobank.org/>”.
388 The authors declare that all other data supporting the findings of this study are
389 available within the paper and its Supplementary Information.

390

391 **Acknowledgements** – We thank J. Montané, E. Aguirre, A. Lacasa, and J.V.
392 Santafé for providing key information on early excavations, and U. Klebe and A.

393 Klebe for transcripts and translation of WGK's field notes. We warmly thank R.
394 Gaete, J. González, E. Nieto, A. Vallès, and I. Fernández for logistics and fossil
395 preparation, and all colleagues who participated in the field campaigns. Eric Gorscak
396 kindly provided XML files for BEAST 2.1.3, B. F. Rotatori assisted with Bayesian
397 phylogenetic methods, and M. Belvedere assisted with photogrammetry techniques.
398 Urs and Anna Klebe gave permission to reproduce WGK and fieldnotes images in
399 Fig. 1 and Suppl. Fig. 2, B. González Riga gave permission to reproduce the skeletal
400 reconstruction in Fig. 1, R. Contreras provided the image for Suppl. Fig. 3, and R.
401 Glasgow reviewed the English. The authors would also like to thank M. C. Lamanna
402 and V. Díez Díaz for their helpful reviews and J. A. Wilson for his constructive
403 feedback on an early version of the manuscript. MNCN provided permissions for
404 study, sampling, and casting the MNCN specimens and Archivo MNCN-CSIC
405 provided permission to reproduce images for Suppl. Figs. 1 and 2.
406 This research is part of the project I+D+i/PID2020-119811GB-I00 funded by MCIN/
407 AEI/10.13039/501100011033/ to B.V. Additional funding was provided by the
408 CERCA Programme and the project CLT009/18/00067 funded by the Generalitat de
409 Catalunya (to B.V. A.S, and A.G.), the Committee for Research and Exploration of
410 the National Geographic Society (grant 9148-12 to B.V.), MEIC, MCI, and MEC
411 (CGL2017-85038-P, CGL2016-77230-P, and CGL2011-30069-C02-01 to A.G., B.V.,
412 A.S., and J.I.C.), and Fundação para a Ciência e a Tecnologia (PTDC/CTA-
413 PAL/31656/2017, UIDB/04035/2020, and PTDC/CTA-PAL/2217/2021 to M.M.A.).
414 Fossil preparation was supported by the Servei de Museus–Departament de Cultura
415 of the Generalitat de Catalunya (grants 2015/104328, CLT005/16/00008,
416 CLT005/19/00045), and the Institut d'Estudis Ilerdencs (grant 201602412).
417

418 **Author contributions**

419 B.V. devised and directed the project and supervised the fieldwork; B.V., A.S., A.G.,
420 N.L.R., and J.I.C. collected the fossils and taphonomic data in the field; B.V, A.S.,
421 and A.G. supervised fossil preparation; B.V. described and measured the fossils,
422 and collected historical information; M.M.A. and B.V. performed phylogenetic and
423 biogeographic analyses; A.G.-D., A.S., and B.V. conducted histological analyses;
424 N.L.R. performed the photogrammetry and 3D modelling; B.V. wrote the paper with
425 substantial inputs of A.S., M.M.A., A.G-D., and N.L.R. B.V., A.S., and M.M.A.
426 designed the figures. B.V., A.S., M.M.A., N.L.R., A.G-D., A.G., and J.I.C. reviewed
427 and edited the original draft.

428

429 **Competing interests** – The authors declare no competing interests.

430

431

432 **FIGURE CAPTIONS**

433

434 **Figure 1. Type locality of *Abditosaurus kuehnei* gen. et sp. nov.** **a**, location of
435 the Orcau-1 locality in the southern Pyrenees (Catalonia, Spain). **b**, the discoverer,
436 Professor Walter Georg Kühne (1911–1991), during a lecture at the Palaeontological
437 Society of Berlin in 1959 (courtesy of Urs and Anna Klebe). **c**, site map showing the
438 skeletal disposition of the *in situ* skeletal elements recovered, mapped, and/or
439 collected during excavations since 1954. The position of the remains discovered in
440 the early excavations is based on sketches from Kühne’s notebook (see
441 Supplementary Section 2.1). **D**, schematic skeletal reconstruction in right lateral
442 view, with indication of the recovered elements (silhouette courtesy of Bernardo
443 González Riga). ?, indeterminate “flat bone”; ca, calcaneum; ch, chevron; co,
444 coracoid; cr, cervical rib; CV, cervical vertebra; dr, dorsal rib; DV, dorsal vertebra; f,

445 femur; fi, fibula; h, humerus; il, ilium; r, radius; sc, scapula; sp, sternal plate; sr,
446 sternal rib; t, tooth; ti, tibia.

447

448 **Figure 2. Skeletal anatomy of *Abditosaurus kuehnei* gen. et sp. nov.** **a**, anterior
449 dorsal and cervical vertebrae (MCD-9882) in ventral view; **b**, third dorsal vertebra
450 (MCD-6718) in posterior view; **c**, fourth and fifth dorsal vertebrae (MCD-6729, MCD-
451 6730) in right ventrolateral view; **d**, second left dorsal rib (MCD-6720) in anterolateral
452 view; **e**, anterior chevron (MNCN-62760) in caudal view; **f**, right scapula (from a cast
453 of MCD-6724) in medial view; **g**, right coracoid (MCD-6742) in lateral view; **h**, left
454 sternal plate (MCD-6716) in ventral view; **i**, sternal rib (MCD-6747) in longitudinal
455 view; **j**, left humerus (MNCN-79834) in anterior view; **k**, right humerus (MCD-6988) in
456 anterior view; **l**, right radius (MCD-6748) in posterior view; **m**, right tibia
457 (MNCN79837-79838-79848) in lateral view; **n**, right fibula (MCD-6723) in lateral
458 view; **o**, left fibula and adhered calcaneum (MNCN-79847) in medial view. acdl,
459 anterior centrodiapophyseal lamina; acpl, anterior centroparapophyseal lamina; al,
460 accessory lamina; ap, acromial plate; aspa, articular surface for ascending process
461 of astragalus; avp, anteroventral process; b, bulge; ca, calcaneum; cap, capitulum;
462 cc, cnemial crest; cdf, centrodiapophyseal fossa; cf, coracoid foramen (twisted
463 mediolaterally); cfo, cnemial fossa; cpor, centropostzygapophyseal fossa
464 (pneumatized); cpol, centropostzygapophyseal lamina; cprl, centroprezygapophyseal
465 lamina; cr, cervical rib; CV, cervical vertebra; d, diapophysis; de, distal end
466 (bevelled); dp, dorsal process; dpc, deltopectoral crest; dr, dorsal rib; DV, dorsal
467 vertebra; gl, glenoid; ior, interosseous ridge; lt, lateral trochanter; pa, parapophysis;
468 pacdf, parapophyseal centrodiapophyseal fossa; pc, pleurocoel; pcdl, posterior
469 centrodiapophyseal lamina; pdr, posterodistal ridge; pf, pneumatic foramen; po,

470 postzygapophysis; pocdf, postzygapophyseal centrodiapophyseal fossa
471 (pneumatized); podl, postzygodiapophyseal lamina; posdf, postzygapophyseal
472 spinodiapophyseal fossa; prcdf, prezygocentrodiapophyseal fossa; pvp,
473 posteroventral process; r, ridge; rac, radial condyle; scb, scapular blade; spdl,
474 spinodiapophyseal lamina; spof, spinopostzygapophyseal fossa; spol,
475 spinopostzygapophyseal lamina; tu, tuberculum; ulc, ulnar condyle. * indicates
476 autapomorphic character. Yellow shading in b indicates a dorsal rib fragment; blue
477 shading in a-c indicates neural arch fossae. Scale bars equal 10 cm.

478

479 **Figure 3. Time-calibrated phylogenetic analysis and palaeobiogeographic**
480 **context of *Abditosaurus kuehnei* gen. et sp. nov. and other saltosaurid**
481 **titanosaurian sauropods.** Plot based on the Maximum Clade Credibility Tree
482 inferred by the tip-dated Bayesian analysis; palaeobiogeographic analysis using the
483 BAYAREALIKE model under starting distribution multipliers. Letters in coloured
484 squares at the nodes indicate relative support for ancestral range reconstruction.
485 Light blue bars represent the 95% highest posterior density for the timing of
486 divergence date at each node. The colour-coded bars for each terminal taxon
487 indicate palaeogeographic range and the 95% highest posterior density of the
488 recorded stratigraphic range of that taxon. Green line indicates the timing of the final
489 breakup and separation between South America and Africa (see Supplementary
490 Section 2.6 for references). Global Polarity Time Scale (GPTS) after Ogg and
491 Hinnov⁵⁸. A, Asia; E, Europe; F, Africa; N, North America; S, South America.

492

493

494

495 **Figure 4. Chronostratigraphy and hypothesized dispersal route for**

496 ***Abditosaurus kuehnei* gen. et sp. nov. and other latest Cretaceous Ibero-**

497 **Armorican titanosaurs. a**, chronostratigraphic range and positions of the Ibero-

498 Armorican titanosaurs and their holotype localities, respectively, correlated to the

499 global sea-level curve, with indication of the timing of the hypothesized dispersal

500 event from Africa to Europe during the KMa2 regressive event. **b**, palaeogeography

501 of the western Tethys Seaway in the early Maastrichtian, with hypothesized

502 migratory pathway (yellow arrow) through the ‘Apulian’ route to the Ibero-Armorican

503 island. Green and yellow boxes represent the chronostratigraphic ranges of the pre-

504 and post-turnover oospecies, respectively. Schemes in circles represent radial thin-

505 sections of *Megaloolithus siruguei* (green circle) and *F. baghensis* (yellow circle)

506 eggshells, taken from Vianey-Liaud et al.⁶⁵. Brackets represent the 95% highest

507 posterior density of the recorded stratigraphic range for each taxon. Ab,

508 *Abditosaurus kuehnei* gen. et sp. nov.; Am, *Ampelosaurus atacis*; At,

509 *Atsinganosaurus velauciensis*; Li, *Lirainosaurus astibiae*; Lo, *Lohuecotitan*

510 *pandafilandi*. HI, Hațeg Island; IB-ARM, Ibero-Armorican Island; NW AFR, north-

511 western Africa. Global Polarity Time Scale (GPTS) after Ogg and Hinnov⁵⁸. Global

512 sea-level curve and eustatic events after Haq⁶¹; sea-level (in m) on top, highstand

513 (left), lowstand (right). Palaeogeographic map based on R. Blakey. Titanosaur

514 silhouette modified from illustrations of O. Sanisidro.

515

516 **REFERENCES**

- 517 1. Le Loeuff, J., Buffetaut, E. & Martin, M. The last stages of dinosaur faunal history
518 in Europe: a succession of Maastrichtian dinosaur assemblages from the
519 Corbières (southern France). *Geol. Mag.* **131**, 625–630 (1994).
- 520 2. Vila, B., Sellés, A. G. & Brusatte, S. L. Diversity and faunal changes in the latest
521 Cretaceous dinosaur communities of southwestern Europe. *Cretaceous Res.* **57**,
522 552–564 (2016).
- 523 3. Fondevilla, V. et al. Chronostratigraphic synthesis of the latest Cretaceous
524 dinosaur turnover in south-western Europe. *Earth Sci. Rev.* **191**, 168–189
525 (2019).
- 526 4. Sanz, J. L., Powell, J. E., Le Loeuff, J., Martínez, R. & Pereda-Suberbiola, X.
527 Sauropod remains from the Upper Cretaceous of Laño (northcentral Spain).
528 Titanosaur phylogenetic relationships. *Estud. Mus. Cienc. Nat. Alava* **14**, 235–
529 255 (1999).
- 530 5. Garcia, G., Amico, S., Fournier, F., Thouand, E. & Valentin, X. A new titanosaur
531 genus (Dinosauria, Sauropoda) from the Late Cretaceous of southern France
532 and its paleobiogeographic implications. *Bull. Soc. Géol. Fr.* **181**, 269–277
533 (2010).
- 534 6. Díez Díaz, V. et al. A new titanosaur (Dinosauria: Sauropoda) from the Upper
535 Cretaceous of Velaux La-Bastide Neuve (southern France). *Hist. Biol.*
536 doi.org/10.1080/08912963.2020.1841184 (2020).
- 537 7. Le Loeuff, J. *Ampelosaurus atacis* (nov. gen., nov. sp.), a new titanosaurid
538 (Dinosauria, Sauropoda) from the Late Cretaceous of the Upper Aude Valley
539 (France). *C. R. Acad. Sci. Paris Serie 2*, **321**, 693–700 (1995).
- 540 8. Díez Díaz, V. et al. A new titanosaur (Dinosauria, Sauropoda) from the Upper
541 Cretaceous of Lo Hueco (Cuenca, Spain). *Cretaceous Res.* **68**, 49–60 (2016).

- 542 9. Company, J. Bone histology of the titanosaur *Lirainosaurus astibiae* (Dinosauria:
543 Sauropoda) from the latest Cretaceous of Spain. *Naturwissenschaften* **98**, 67–78
544 (2011).
- 545 10. Klein, N. et al. Modified laminar bone in *Ampelosaurus atacis* and other
546 titanosaurs (Sauropoda): implications for life history and physiology. *PLoS ONE*
547 **7**, e36907 (2012).
- 548 11. Díez Díaz, V. et al. The titanosaurian dinosaur *Atsinganosaurus velauciensis*
549 (Sauropoda) from the Upper Cretaceous of southern France: new material,
550 phylogenetic affinities, and palaeobiogeographical implications. *Cretaceous Res.*
551 **91**, 429–456 (2018).
- 552 12. Benítez-López, A., Santini, L., Gallego-Zamorano, J., Milá, B., Walkden, P.,
553 Huijbregts, M. A. J. & Tobias, J. A. The island rule explains consistent patterns of
554 body size evolution in terrestrial vertebrates. *Nat. Ecol. Evol.* **5**, 768–786 (2021).
- 555 13. Benton, M. J. et al. Dinosaurs and the island rule: the dwarfed dinosaurs from
556 Hațeg Island. *Palaeogeogr. Palaeoclimatol. Palaeoecol.* **293**, 438–454 (2010).
- 557 14. Canudo, J. I. in Proc. XVII Jornadas de la Sociedad Española de Paleontología
558 (eds Meléndez, G. et al.) 225-262 (Sociedad Española de Paleontología y Área
559 y Museo de Paleontología de la Universidad de Zaragoza, 2001).
- 560 15. Vila, B. et al. The diversity of sauropods and their first taxonomic succession
561 from the latest Cretaceous of south-western Europe: clues to demise and
562 extinction. *Palaeogeogr. Palaeoclimatol. Palaeoecol.* **350-352**, 19–38 (2012).
- 563 16. Sallam, H. M. et al. New Egyptian sauropod reveals Late Cretaceous dinosaur
564 dispersal between Europe and Africa. *Nat. Ecol. Evol.* **2**, 445–451 (2018).
- 565 17. Buffetaut, E. Archosaurian reptiles with Gondwanan affinities in the Upper
566 Cretaceous of Europe. *Terra Res.* **1**, 69–74 (1989).

- 567 18. Le Loeuff, J. The Campano-Maastrichtian vertebrate faunas from southern
568 Europe and their relationships with other faunas in the world;
569 palaeobiogeographical implications. *Cretaceous Res.* **12**, 93–114 (1991).
- 570 19. Pereda-Suberbiola, X. Biogeographical affinities of Late Cretaceous continental
571 tetrapods of Europe: a review. *Bull. Soc. Geol. Fr.* **180**, 57–71 (2009).
- 572 20. Csiki-Sava, Z., Buffetaut, E., Ósi, A., Pereda-Suberbiola, X. & Brusatte, S. L.
573 Island life in the Cretaceous – faunal composition, biogeography, evolution, and
574 extinction of land-living vertebrates on the Late Cretaceous European
575 archipelago. *ZooKeys* **469**, 1–161 (2015).
- 576 21. Ezcurra, M. D. & Agnolín, F. L. A new global palaeobiogeographical model for
577 the late Mesozoic and early Tertiary. *Syst. Biol.* **61**, 553–566 (2012).
- 578 22. Sellés, A. G. & Vila, B. Re-evaluation of the age of some dinosaur localities from
579 the southern Pyrenees by means of megaloolithid oospecies. *J. Iber. Geol.* **41**,
580 125–139 (2015).
- 581 23. Bonaparte, J. F. & Coria, R. A. Un nuevo y gigantesco saurópodo titanosaurio de
582 la Formación Río Limay (Albiano–Cenomaniano) de la Provincia del Neuquén,
583 Argentina. *Ameghiniana* **30**, 217–282 (1993).
- 584 24. Curry Rogers, K. The postcranial osteology of *Rapetosaurus krausei*
585 (Sauropoda: Titanosauria) from the Late Cretaceous of Madagascar. *J. Vertebr.*
586 *Paleontol.* **29**, 1046–1086 (2009).
- 587 25. Zurriaguz, V. & Powell, J. New contributions to the presacral osteology of
588 *Saltasaurus loricatus* (Sauropoda, Titanosauria) from the Upper Cretaceous of
589 northern Argentina. *Cretaceous Res.* **54**, 283–300 (2015).
- 590 26. Coria, R. A., Filippi, L. S., Chiappe, L. M., García, R. & Arcucci, A. B.
591 *Overosaurus paradasorum* gen. et sp. nov., a new sauropod dinosaur

- 592 (Titanosauria: Lithostrotia) from the Late Cretaceous of Neuquén, Patagonia,
593 Argentina. *Zootaxa* **3683**, 357–376 (2013).
- 594 27. Calvo, J. O., González Riga, B. J. & Porfiri, J. D. A new titanosaur sauropod from
595 the Late Cretaceous of Neuquén, Patagonia, Argentina. *Arquivos do Museu*
596 *Nacional, Rio de Janeiro* **65**, 485–504 (2007).
- 597 28. Jain, S. L. & Bandyopadhyay, S. New titanosaurid (Dinosauria: Sauropoda) from
598 the Late Cretaceous of central India. *J. Vertebr. Paleontol.* **17**, 114–136 (1997).
- 599 29. Gorscak E. & O'Connor P. M. A new African titanosaurian sauropod dinosaur
600 from the middle Cretaceous Galula Formation (Mtuka Member), Rukwa Rift
601 Basin, southwestern Tanzania. *PLoS ONE* **14**, e0211412 (2019).
- 602 30. Kellner, A. W. A. & de Azevedo, S. A. K. A new sauropod dinosaur
603 (Titanosauria) from the Late Cretaceous of Brazil. *Nat. Sci. Mus. Monogr.* **15**,
604 111–142 (1999).
- 605 31. Novas, F. E. et al. Paleontological discoveries in the Chorrillo Formation (upper
606 Campanian-lower Maastrichtian, Upper Cretaceous), Santa Cruz Province,
607 Patagonia, Argentina. *Rev. Mus. Argentino Cienc. Nat.* **21**, 217–293 (2019).
- 608 32. Wilson, J. A., D'Emic, M. D., Curry Rogers, K. A., Mohabey, D. M. & Sen, S.
609 Reassessment of the sauropod dinosaur *Jainosaurus* (=“*Antarctosaurus*”)
610 *septentrionalis* from the Upper Cretaceous of India. *Contrib. Mus. Paleontol.,*
611 *University of Michigan*, **32**, 17–40 (2009).
- 612 33. Powell, J. E. Revision of South American titanosaurid dinosaurs:
613 palaeobiological, palaeobiogeographical and phylogenetic aspects. *Records of*
614 *the Queen Victoria Museum* **111**, 1–173 (2003).
- 615 34. Smith, J. B. et al. A giant sauropod dinosaur from an Upper Cretaceous
616 mangrove deposit in Egypt. *Science* **292**, 1704–1706 (2001).

- 617 35. Otero, A. & Vizcaíno, S. F. Hindlimb musculature and function of *Neuquensaurus*
618 *australis* (Sauropoda: Titanosauria). *Ameghiniana* **45**, 333-348 (2008).
- 619 36. Huene, F. von. Los saurisquios y ornitisquios del Cretáceo Argentino. *An. Mus.*
620 *La Plata* **3**, 1–196 (1929).
- 621 37. Mannion, P.D. & Otero, A. A reappraisal of the Late Cretaceous Argentinean
622 sauropod dinosaur *Argyrosaurus superbis*, with a description of a new
623 titanosaur genus. *J. Vertebr. Paleontol.* **32**, 614–638 (2012).
- 624 38. Mocho, P., Pérez-García, A., Martín Jiménez, M. & Ortega, F. New remains from
625 the Spanish Cenomanian shed light on the Gondwanan origin of European Early
626 Cretaceous titanosaurs. *Cretaceous Res.* **95**, 164–190 (2019).
- 627 39. Díez Díaz, V., Pereda Suberbiola, X. & Sanz, J. L. Appendicular skeleton and
628 dermal armour of the Late Cretaceous titanosaur *Lirainosaurus astibiae*
629 (Dinosauria: Sauropoda) from Spain. *Palaeontol. Electron.* **16**, 19A (2013).
- 630 40. Le Loeuff, J. in *Thunder-Lizards: The Sauropodomorph Dinosaurs* (eds Tidwell,
631 V. & Carpenter, K.) 115–137 (Indiana Univ. Press, Bloomington, 2005).
- 632 41. Borsuk-Bialynicka, M. A new camarasaurid sauropod *Opisthocoelicaudia*
633 *skarzynskii* gen. n., sp. n. from the Upper Cretaceous of Mongolia. *Palaeontol.*
634 *Pol.* **37**, 5–63 (1977).
- 635 42. Filippi, L. S., García, R. A. & Garrido, A. A new sauropod titanosaur from the
636 Plottier Formation (Upper Cretaceous) of Patagonia (Argentina). *Geol. Acta* **9**, 1–
637 12 (2011).
- 638 43. Salgado, L., Coria, R. A. & Calvo, J. O. Evolution of titanosaurid sauropods. I:
639 Phylogenetic analysis based on the postcranial evidence. *Ameghiniana* **34**, 3–32
640 (1997).

- 641 44. D’Emic, M. D. The early evolution of titanosauriform sauropod dinosaurs. *Zool. J.*
642 *Linn. Soc.* **166**, 624–671 (2012).
- 643 45. Tschopp, E. & Mateus, O. Clavicles, interclavicles, gastralia, and sternal ribs in
644 sauropod dinosaurs: new reports from Diplodocidae and their morphological,
645 functional and evolutionary implications. *J. Anat.* **222**, 321–340 (2013).
- 646 46. Wilson, J. A. Sauropod dinosaur phylogeny: critique and cladistic analysis. *Zool.*
647 *J. Linn. Soc.* **136**, 217–276 (2002).
- 648 47. Powell, J. E. in *Los dinosaurios y su entorno biótico* (eds Sanz, J. L. &
649 Buscalioni, A. D.) 165–230 (Instituto ‘Juan de Valdés’, 1992).
- 650 48. Otero, A. The appendicular skeleton of *Neuquensaurus*, a Late Cretaceous
651 saltosaurine sauropod from Patagonia, Argentina. *Acta Palaeontol. Pol.* **55**, 399–
652 426 (2010).
- 653 49. Gilmore, C. W. Reptilian fauna of the North Horn Formation of central Utah.
654 *Geol. Surv. Prof. Paper* **210**, 1–52 (1946).
- 655 50. Ullmann, P. V. & Lacovara, K. J. Appendicular osteology of *Dreadnoughtus*
656 *schrani*, a giant titanosaurian (Sauropoda, Titanosauria) from the Upper
657 Cretaceous of Patagonia, Argentina. *J. Vertebr. Paleontol.* **36**, e1225303 (2016).
- 658 51. Poropat, S. F. Carl Wiman’s sauropods: the Uppsala Museum of Evolution’s
659 collection. *GFF* **135**, 104–119 (2013).
- 660 52. Cerda, I. A., Salgado, L. & Powell, J. E. Extreme postcranial pneumaticity in
661 sauropod dinosaurs from South America. *Paläontologische Zeitschrift* **86**, 441–
662 449 (2012).
- 663 53. Wilson, J. A. & Carrano, M. T. Titanosaurs and the origin of “wide-gauge”
664 trackways: a biomechanical and systematic perspective on sauropod locomotion.
665 *Paleobiol.* **25**, 252–267 (1999).

- 666 54. Upchurch, P., Barrett, P. & Dodson, P. in *The Dinosauria* (eds Weishampel, D.
667 B., Dodson, P. & Osmólska, H) 259–324 (Univ. California Press, 2004).
- 668 55. Lehman, T. M. & Coulson, A. B. A juvenile specimen of the sauropod dinosaur
669 *Alamosaurus sanjuanensis* from the Upper Cretaceous of Big Bend National
670 Park, Texas. *J. Paleontol.* **76**, 156–172 (2002).
- 671 56. Gallina, P. A. & Otero, A. Reassessment of *Laplatasaurus araukanicus*
672 (Sauropoda: Titanosauria) from the Upper Cretaceous of Patagonia, Argentina.
673 *Ameghiniana* **52**, 487–501 (2015).
- 674 57. Wilson, J. A. & Upchurch, P. Redescription and reassessment of the
675 phylogenetic affinities of *Euhelopus zdanskyi* (Dinosauria: Sauropoda) from the
676 Early Cretaceous of China. *J. Syst. Palaeontol.* **7**, 199–239 (2009).
- 677 58. Ogg, J. G. & Hinnov, L. A. in *The Geological Time Scale* (eds Gradstein, F. M. et
678 al.) 793–853 (Elsevier, 2012).
- 679 59. Sereno, P. C. A rationale for phylogenetic definitions, with application to the
680 higher-level taxonomy of Dinosauria. *Neues Jahrb. Geol. Paläontol. Abh.* **210**,
681 41–83 (1998).
- 682 60. Chiappe, L. M., Coria, R. A., Dingus, L., Jackson, F., Chinsamy, A. & Fox, M.
683 Sauropod dinosaur embryos from the Late Cretaceous of Patagonia. *Nature* **396**,
684 258–261 (1998).
- 685 61. Haq, B. U. Cretaceous eustasy revisited. *Glob. Planet. Change* **113**, 44–58
686 (2014).
- 687 62. Gheerbrant, E. & Rage, J. -C. Paleobiogeography of Africa: how distinct from
688 Gondwana and Laurasia? *Palaeogeogr. Palaeoclimatol. Palaeoecol.* **241**, 224–
689 246 (2006).

- 690 63. Canudo, J. I. et al. What Iberian dinosaurs reveal about the bridge said to exist
691 between Gondwana and Laurasia in the Early Cretaceous. *Bull. Soc. Géol. Fr.*
692 **180**, 5–11 (2009).
- 693 64. Dal Sasso, C., Pierangelini, G., Famiani, F., Cau, A. & Nicosia, U. First sauropod
694 bones from Italy offer new insights on the radiation of Titanosauria between
695 Africa and Europe. *Cretaceous Res.* **64**, 88–109 (2016).
- 696 65. Vianey-Liaud, M., Khosla, A. & Garcia, G. Relationships between European and
697 Indian dinosaur eggshells of the oofamily Megaloolithidae. *J. Vertebr. Paleontol.*
698 **23**, 575–585 (2003).
- 699 66. Stein, K. et al. Small body size and extreme cortical bone remodeling indicate
700 phyletic dwarfism in *Magyarosaurus dacus* (Sauropoda: Titanosauria). *Proc.*
701 *Natl. Acad. Sci. USA* **107**, 9258–9263 (2010).
- 702 67. Botfalvai, G. et al. ‘X’ marks the spot! Sedimentological, geochemical and
703 palaeontological investigations of Upper Cretaceous (Maastrichtian) vertebrate
704 fossil localities from the Vălioara valley (Densuş-Ciula Formation, Haţeg Basin,
705 Romania). *Cretaceous Res.* **123**, 104781 (2021).
- 706 68. Csiki-Sava, Z. et al. The east side story—the Transylvanian latest Cretaceous
707 continental vertebrate record and its implications for understanding Cretaceous–
708 Paleogene boundary events. *Cretaceous Res.* **57**, 662–698 (2016).
- 709 69. Campione, N. E. & Evans, D. C. A universal scaling relationship between body
710 mass and proximal limb bone dimensions in quadrupedal terrestrial tetrapods.
711 *BMC Biology* **10**, 60 (2012).
- 712 70. González Riga, B. J., Lamanna, M. C., Ortiz David, L. D., Calvo, J. O. & Coria, J.
713 P. A gigantic new dinosaur from Argentina and the evolution of the sauropod
714 hind foot. *Sci. Rep.* **6**, 19165 (2016).

- 715 71. Seebacher, F. New method to calculate allometric length-mass relationships of
716 dinosaurs. *J. Vertebr. Paleontol.* **21**, 51–60 (2001).
- 717 72. Mallison, H. & Wings, O. Photogrammetry in paleontology— a practical guide. *J*
718 *Paleontol Tech.* **12**, 1–31 (2014).
- 719 73. Matthews, N., Noble, T. & Breithaupt, B. H. in *Dinosaur Tracks—The Next Steps*
720 (eds Falkingham, P. L. et al.) 28–55 (Indiana University Press, 2016).
- 721 74. Falkingham, P. L. et al. A standard protocol for documenting modern and fossil
722 ichnological data. *Palaeontology* **61**, 469–480 (2018).
- 723 75. Huelsenbeck, J. P. & Ronquist, F. 2001. MRBAYES: Bayesian inference of
724 phylogeny. *Bioinformatics* **17**, 754–755 (2001).
- 725 76. Stadler, T., Kühnert, D., Bonhoeffer, S. & Drummond, A. J. Birth-death skyline
726 plot reveals temporal changes of epidemic spread in HIV and hepatitis C virus
727 (HCV). *Proc. Natl. Acad. Sci. USA.* **110**, 228–233 (2013).
- 728 77. Matzke, N. J. Probabilistic historical biogeography: new models for founder-
729 event speciation, imperfect detection, and fossils allow improved accuracy and
730 model-testing. *Front. Biogeogr.* **5**, 242–248 (2013).

